The Experimental Validation and Application of CFD and CMFD Codes in Nuclear Reactor Technogy
OECD/NEA & International Atomic Energy Agency (IAEA) Workshop
Daejeon, Korea, 10–12 September 2012

CFD MODEL OF WALL BOILING INCLUDING A POPULATION BALANCE MODEL

Eckhard Krepper, Roland Rzehak
Helmholtz-Zentrum Dresden-Rossendorf e. V.
Institute of Fluid Dynamics, 01314 Dresden, Germany, www.hzdr.de
E.Krepper@hzdr.de

Conxita Lifante, Thomas Frank
ANSYS Germany GmbH, Germany -83624 Otterfing, Staudenfeldweg 12
www.ansys.com

Keywords: CFD, two phase flow, wall boiling, population balance model, experiments, model validation

Abstract
In this work the present capabilities of CFD for wall boiling are investigated. The computational model is based on the Euler / Euler two-phase flow description with heat flux partitioning. In the framework of interpenetrating continua the exchange of momentum, mass and energy between the phases are essential. The description of the interfacial morphology plays an important role. In the actual work a population balance model for the description of the gaseous phase considering bubble coalescence, bubble fragmentation and bubble size changes caused by condensation of evaporation is applied. The wall boiling model is coupled with the population balance model.
For the demonstration, DEBORA tests (Garnier, 2001) were used. In the DEBORA tests in a vertical tube Dichlorodifluoromethane (R12) was heated from the side walls. Radial profiles for gas volume fraction, gas velocity, liquid temperature and bubble size were measured.
The results show the potential of this model approach which is able to describe the observed bubble size increase after leaving the wall as well as the change of gas volume fraction profile from wall to core peaking with increasing inlet temperature.

1. INTRODUCTION

In Nuclear Reactor Technology, the understanding and capability of modelling boiling processes are of fundamental importance for the safe and effective operation of the plant. One essential application example is the simulation of a hot channel of a fuel element. Here the secure control of avoiding critical heat flux is essential. Expensive experiments can be complemented or even replaced by simulations. Only CFD methods are able to simulate the phenomena independent on the certain geometry. The correct simulation of subcooled boiling as a preliminary phase for critical heat flux is an essential step towards the simulation of critical heat flux.
For engineering calculations, currently the most widely used CFD approach to model two-phase flows with significant volume fractions of both phases is the Eulerian two-fluid framework of interpenetrating continua. In this approach, balance equations for mass, momentum and energy are written for each phase, i.e. gas and liquid, separately and weighted by the so-called volume-fraction which represents the ensemble averaged probability of occurrence for each phase at a certain point in time and space. Exchange terms between the phases appear as source / sink terms in the balance equations. The exchange between the phases is mainly influenced by the interfacial morphology. Up to medium values of the gas volume fraction, the two-phase flow is in the bubbly flow regime. In this instance, the mass and momentum exchange between the phases is conveniently parametrized by the bubble size. To account for deformations the equivalent spherical diameter is used as a measure of bubble size. Earlier analyses of boiling tests simulate the bubble size monodispersed algebraic dependent on the liquid temperature.

Experimental investigations have shown that forces acting on the bubbles depend on the bubble size. The effect is most severe for the lift force which even changes its direction at a certain bubble size that depends on the fluid properties. To capture this behaviour separate momentum equations are required for bubbles of different size. For this reason the so-called inhomogeneous-MUSIG (MUltiple SIze Group) model was developed (e.g. Frank et al. 2008). In flows with phase change, besides coalescence and fragmentation condensation and evaporation provide additional mechanisms for the evolution of bubble size. Corresponding extensions of the MUSIG model to consider heat and mass transfer were formulated (Lucas et al. 2011). The recent coupling of the wall boiling model with the population balance model describes the bubble generated at a heated wall with a certain size that subsequently evolves due to both coalescence / fragmentation and condensation / evaporation processes (Lifante et al. 2011).
The present paper describes the capabilities of this CFD approach by means of DEBORA tests (Garnier, 2001). In the DEBORA tests Dichlorodifluoromethane (R12) was applied as the working fluid, avoiding conditions inconvenient for measurements in a hot channel of water at high pressure and high temperatures. Radial profiles for gas volume fraction, gas velocity, liquid temperature and bubble size were measured.

2. THE EXPERIMENTS

A detailed description of the DEBORA test facility can be found in Manon (2000) and Garnier et al. (2001). In a vertical pipe having an inner diameter of 19.2 mm Dichlorodifluoromethane (R12) is heated over a pipe length of 3.5 m. The facility is operated with mass flow rates of 2000 to 3000 kg/m^2/s at a system pressure of 1.46 to 2.62 MPa. The radial profiles for gas volume fraction and gas velocity at the end of the heated length are measured by means of an optical probe. Furthermore, profiles of bubble size at this position are available. In addition, radial liquid temperature profiles as well as axial profiles of the wall temperature are measured by thermocouples.
Table 1 lists the parameters of the DEBORA tests selected for the present investigation. DEBORA 1 corresponds to a test considered by several previous authors e.g. Manon (2000), Yao and Morel (2002) and Boucker et al (2006). The test DEBORA 2 has an increased inlet temperature and was investigated also by Yao and Morel (2002). The tests DEBORA 3 to DEBORA 7 represent a series of tests at lower pressure having the same mass flow rate and wall heat flux but increasing inlet temperature. Here, DEBORA 7 represents the extreme case with maximum vapour generation. In the experiments a shift of the radial gas volume fraction profile from wall peaking (DEBORA 3) to core peaking (DEBORA 7) was determined. The question is, whether the tendencies found in the tests can also be reproduced in the simulations.

Table 1: System parameters for the selected test cases.

	Pressure [MPa]	Mass flow rate [kg m^{-2} s^{-1}]	Wall heat flux [kW m^{-2}]	Inlet tempe-rature [°C]	outlet equilibrium vapour quality	Test No
DEBORA 1	2.62	1996	73.89	68.52	0.058	29G2P26W16Te68
DEBORA 2	2.62	1985	73.89	70.53	0.0848	29G2P26W16Te70
DEBORA 3	1.46	2028	76.2	28.52	-0.0279	29G2P14W16Te27.3
DEBORA 4	1.46	2030	76,24	31,16	-0.0071	29G2P14W16Te30
DEBORA 5	1.46	2028	76.19	35.6	0.0319	29G2P14W16Te34.5
DEBORA 6	1.46	2023	76.26	39.67	0.0687	29G2P14W16Te38.8
DEBORA 7	1.46	2024	76.26	44,21	0.1091	29G2P14W16Te43.5

3. THE MODELS

The general equations for diabatic two-phase flow in the Euler/Euler framework of interpenetrating continua have been reviewed in many places before. Therefore, the description here is focussed on those issues that are particularly relevant for the present investigation. The subcooled boiling model implemented in ANSYS CFX has been used in a large number of previous studies.

The first issue is the wall boiling model describing vapour generation at the wall and transfer of sensible heat to the liquid. Here, the CFX model closely follows the heat flux partitioning approach of Kurul and Podowski (1990, 1991). It has been emphasized in Krepper and Rzehak (2011) that some of the commonly used correlations are not universally applicable but have to be recalibrated carefully to the specific conditions under investigation.

A second issue is the modelling of interfacial area that determines the exchange of mass, momentum and energy between the phases. For the bubbly flow regime it is convenient to use an equivalent Sauter diameter and work with the bubble size. In boiling flows the bubble size may change due to both bubble coalescence / breakup and condensation / evaporation. In the present paper a distribution of bubble sizes is considered which varies dynamically as described by a population balance model with a source at the wall, the size of the generated bubbles being given by the bubble detachment diameter as calculated from the wall boiling model. This allows to include also the important processes of bubble coalescence and breakup in the model. Since the corresponding rates depend sensitively on the turbulence, special attention has to be given to the modelling of bubble induced contributions to the turbulence. To simplify matters, the vapour bubbles are assumed to be at saturation temperature everywhere which is a rather good approximation except close to the critical heat flux.

Turbulent fluctuations are modelled by a shear stress turbulence (SST) model according to Menter (1994) applied to the liquid phase. This corresponds to a $k - \omega$ model near the walls and a $k - \varepsilon$ model far from walls. The frequently used prescription of Sato (1981) for the bubble induced turbulence has been replaced by including source terms in the turbulence equations following Politano et al. (2003). In addition, a wall function for boiling flows based on analogy to a rough wall is employed, which could be shown in Krepper and Rzehak (2011) to give an improved prediction of the velocity profiles.

For momentum exchange between the phases, finally, lift and turbulent dispersion forces are included in the model in addition to the ubiquitous drag force. There is in addition also a force that pushes a bubble translating in an otherwise quiescent liquid parallel to a wall in close proximity away from this wall. Different models for this so-called wall force were investigated but the influence turned out to be small. Therefore in the present study this force was neglected. In general the applicability of a wall force to flow boiling should be investigated further.

3.1. Wall boiling model

The given external heat flux Q_{tot}, applied to the heated wall is written as a sum of three parts:

$$Q_{tot} = Q_C + Q_Q + Q_E \tag{1}$$

where Q_C, Q_Q and Q_E denote the heat flux components due to single-phase turbulent convection, quenching, and evaporation, respectively. The individual components in this heat flux partitioning are then modelled as functions of the wall temperature and other local flow parameters. Once this is accomplished, Eq. (1) can be solved iteratively for the local wall temperature T_W, which satisfies the wall heat flux balance.

Sensitivity studies have shown the bubble size at detachment and the nucleation site density are parameters with strong influence on the calculated results. The bubble size at detachment depends on the liquid subcooling. Also the liquid properties, the system pressure and the heat flux have an influence. Finally the mechanical attraction of the surrounding flow, as indicated by the fluid velocity determines the detachment of a growing bubble.

An investigation of the bubble size at detachment was performed by Tolubinsky and Kostanchuk (1970) for water at different pressures and subcoolings. The observed dependence on the liquid subcooling at atmospheric pressure can be fitted to a correlation

$$d_W = d_{ref} e^{-\frac{T_{sat}-T_L}{\Delta T_{redf}}} \tag{2}$$

where T_L is determined by is obtained by evaluating the non-dimensional temperature profile of Kader (1981) at a fixed value of y^+.
The situation concerning data on nucleation site density is much less clear. Most of the time, correlations are expressed in the form of power laws depending on the wall superheat as

$$N = N_{ref}\left(\frac{T_W - T_{sat}}{\Delta T_{refN}}\right)^p \tag{3}$$

In terms of bubble detachment diameter and nucleation site density given by Eqs. (2) and (3) the wall area fraction influenced by vapour bubbles A_W, is given by

$$A_W = \pi\left(a\frac{d_W}{2}\right)^2 N \tag{4}$$

Here, a is the so-called bubble influence factor, for which a value of 2 is commonly used (Kurul and Podowski 1990, 1991). Direct experimental evidence concerning this quantity is rather scarce. Probably the most relevant source is Han (1965) who in some „rough“ experiments determined the hydrodynamic disturbance caused by lifting a spherical particle from a horizontal surface and found that it has a range of twice the size of the particle. A similar size has been claimed by Cieslinski (2005) from PIV measurement of the flow field around departing bubbles, although the quality of the images presented is rather poor.
Since $A_W = 1$ corresponds to the case where the whole surface is under the influence of bubbles, A_W as calculated by Eq. (4) has to be limited to values smaller than this limit. Moreover, it should be kept in mind that already as A_W approaches 1 the assumptions of the model are not really satisfied anymore.

3.2. Population balance approach to bubble size distribution

To describe polydispersed flows within a purely Eulerian approach, a number of different (MUltiple) bubble SIze Groups i = 1 … M is considered, each representing bubbles of typical size d_i. The fraction of gas volume contained in each bubble size group is denoted as α_i so that the total gas volume fraction is given by

$$\alpha_G = \sum_{i=1}^{M} \alpha_i \tag{5}$$

It is useful to also define occupation numbers $f_i = \alpha_i / \alpha_G$ giving the contribution of each size group to the total gas volume fraction. Obviously we then have $\Sigma_i f_i = 1$.

For each size group the equation of mass conservation assumes the form

$$\frac{\partial}{\partial t}(\alpha_i \rho_G) + \nabla(\alpha_i \rho_G \mathbf{u}_G) = \Gamma_i^{topo} + \Gamma_i^{phase} \tag{6}$$

where the right hand side gives the net source of mass for group *i* which results from topological changes due to coalescence and breakup as well as phase change due to condensation and evaporation. Models for these two contributions will be discussed in the following subsections.

For the homogeneous MUSIG model only one momentum and energy equation for the total amount of vapour is considered as well as the conservation equations of the liquid of course. In these equations the total gas volume fraction α_G is calculated according to Eq. (5) above. In addition, also the bubble size d_B appears which is taken in the Sauter sense representing the interfacial area $A_I = 6\ \alpha_G / d_B$. In order to preserve this interpretation, d_B is calculated from the occupation number and bubble size for each group as

$$d_B = \left(\sum_{i=1}^{M} \frac{f_i}{d_i} \right)^{-1} \tag{7}$$

The advantage of the homogeneous MUSIG approach is that a large number of bubble size groups can be considered while keeping the computational effort within reasonable bounds. On the other hand profound effects of bubble size are missed entirely like for example the change in the sign of the lift force as shown in Fig. 2. To capture such phenomena, provision has to be made that bubbles of different size may move with different velocities.

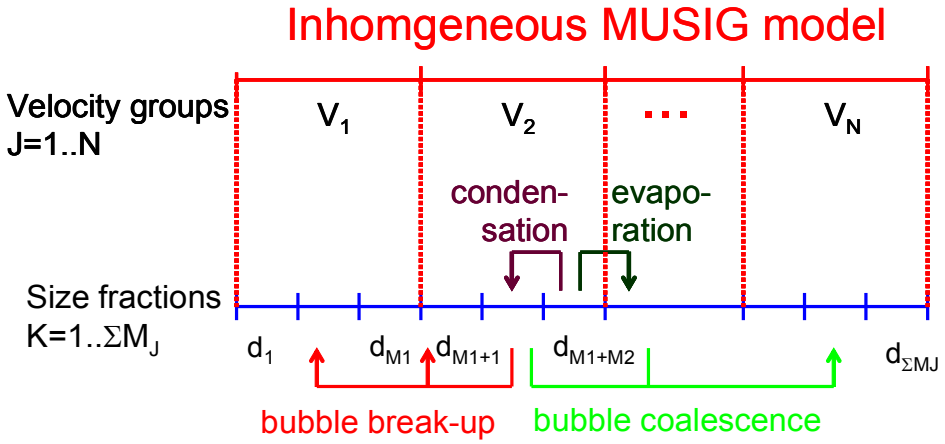

Figure 1: Principle schema of the inhomogeneous MUSIG model including phase transfer

The inhomogeneous MUSIG model (Frank et al. 2008, Krepper et al. 2008) was developed to overcome these limitations. In the extreme case a full set of conservation laws would be solved for each size group each containing the individual volume fraction α_i and bubble size d_i. Such an approach is infeasible, however, for a number of 20 to 30 size groups as required for a realistic description. Therefore, a smaller number N < M of velocity groups is chosen, each of which is assigned to a range of adjacent size groups as shown schematically in Fig. 1. For each of these, the sums in the birth and death rates are extended only over the range of assigned size groups. In this way computational effort and accurate representation can be balanced according to the requirements of a specific application. Often a minimum value of N = 2 is already found to give acceptable results.
When condensation or evaporation occur, the volume fraction in size group *i* changes since mass is transferred directly between the bubbles and the liquid and since due to this direct mass transfer the bubbles are shrinking or growing they may subsequently belong to a different size group. Written as a source term for size group *i* the direct mass transfer to the liquid is given by

$$\tilde{\Gamma}_i = -\frac{A_{I,i}}{H_{LG}} h_{L,i} (T_L - T_{sat}) \tag{8}$$

The procedure is more detailed described by Lucas et al. 2011. The assumption has been made that the gas is at saturation temperature.This formulation is extended in order to couple this polydisperse approach to the wall boiling model (Lifante et al. 2011). The coupling consists actually in the inclusion of one more source term, S_{rpi}, in eq. (8) only for the size fraction equation corresponding to the class whose diameter is the closest to the bubble departure diameter d_W.
In the present work bubble coalescence and breakup are described by the models proposed by Prince and Blanch (1990) and by Luo and Svendsen (1996). To obtain agreement with the measurements, efficiency factors F_C and F_B were introduced and calibrated to match the measured radial bubble size profiles. This procedure was successful in so far as all tests at the same pressure could be calculated with the same set of calibration parameters (see Table. 3). Of course, this has to be considered only as a first step and further model development needs to be done.

3.3. Momentum transfer

An essential element of the Euler/Euler framework of interpenetrating continua is the description of the momentum transfer between continuous liquid and dispersed gas. For momentum exchange between the phases, the Ishii and Zuber (1979) drag law was used. A Favre averaged turbulence dispersion force (Burns et al. 2004) were included. A more detailed description of the momentum transfer models was given by Krepper and Rzehak (2011). As noted in the publication, the effect of an additional wall force is small. Therefore in the present study this force was neglected. In the following expressions, the forces for the dispersed gaseous phase are given.
Furthermore, a lift force according to Tomiyama et al. (2002) was considered. Whereas most of the considered forces show only a quite weak dependency on the bubble size a different situation is found for the lift force. Here the force with increasing bubble size changes even the sign. The inhomogeneous MUSIG model enables at least a rough consideration of the dependency of the momentum transfer on the bubble size by introduction of different velocity fields.
The corresponding momentum source for the lift force is given by

$$\mathbf{F}^{lift} = -C_L \rho_L \alpha_G (\mathbf{u}_G - \mathbf{u}_L) \times rot(\mathbf{u}_L) \tag{8}$$

Experimental (Tomiyama et al. 2002) and numerical (Schmidtke, 2008) investigations showed that the direction of the lift force changes its sign, if a substantial deformation of the bubble occurs. From the observation of the trajectories of single bubbles rising in simple shear flow of a glycerol water solution the following correlation for the lift coefficient was derived:

$$C_L = \begin{cases} \min[0.288\tanh(0.121\mathrm{Re}), f(Eo_\perp)] & Eo_\perp < 4 \\ f(Eo_\perp) & for \quad 4 < Eo_\perp < 10 \\ -0.27 & 10 < Eo_\perp \end{cases} \tag{9}$$
$$with \quad f(Eo_\perp) = 0.00105 Eo_\perp^3 - 0.0159 Eo_\perp^2 - 0.0204 Eo_\perp + 0.474$$

This coefficient depends on the modified Eötvös number given by:

$$Eo_\perp = \frac{g(\rho_L - \rho_G) d_\perp^2}{\sigma} \tag{10}$$

Here $d_\perp$ is the maximum horizontal dimension of the bubble. It is calculated using an empirical correlation for the aspect ratio by the following equation (Wellek et. al 1966):

$$d_\perp = d_B \sqrt[3]{1 + 0.163 \; Eo^{0.757}} \tag{11}$$

For the water-air system at normal conditions C_L changes its sign at d_B = 5.8 mm which was confirmed by investigations of polydispersed upward vertical air/water bubbly flow (Lucas et. al 2007b, 2007c). For R12 this value is decreased substantially to about 1.5 mm at 1.46 MPa and about 1.0 mm at 2.65 MPa, respectively, as shown in Fig. 2.

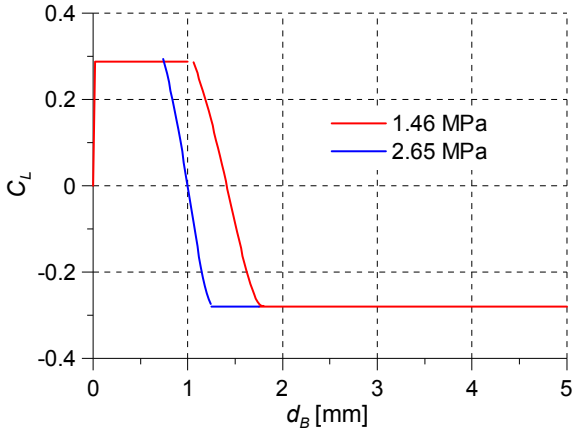

Figure 2: Dependency of the lift coefficient C_L on the bubble size d_B for R12 according to Eq. (9) with material properties for R12.

Applying the inhomogeneous MUSIG approach the changing sign of the lift force can be simulated by consideration of at least two different velocity fields for small and large bubbles.

4. SETUP

4.1. General setup

The tests were simulated in a quasi-2D cylindrical geometry, i.e. a narrow cylindrical sector with symmetry boundary conditions imposed on the side faces. The validity of this simplification has been verified by grid resolution studies and by comparison to a 3D simulation representing a 60° sector of the pipe. An inlet condition was set at the bottom. The inlet profile for the liquid flow was set according to a typical turbulent flow profile in a pipe. At the outlet at the top a pressure boundary condition was imposed.

For R12 liquid and vapour the relevant material properties were taken from the National Institute of Standards and Technology (NIST) Standard Reference Database on Thermophysical Properties of Fluid Systems (http://webbook.nist.gov/chemistry/fluid). Fluid property tables based on these data were generated and used in the calculations.

On the heated walls, boundary conditions for mass and energy equations are provided by the heat flux partitioning discussed in section 3. It remains to specify boundary conditions for the gas and liquid momentum equations. Since the gas volume fraction in our model represents bubbles that have detached from the wall, an appropriate boundary condition for the gas phase is the free slip condition. For the liquid phase we argue that bubbles which have not left the wall are still attached to their respective nucleation site. Hence they restrain the liquid motion in the same way as the solid wall itself does. Therefore we choose a no-slip condition for the liquid phase. While this issue does not appear to have received due attention in the literature, the results to be presented justify our choice as preliminary working solution until a more thorough investigation becomes available.

All of these two phase flow simulations have been carried out on a quite coarse grid for which the centre of the grid cells adjacent to the wall has a non-dimensional coordinate of y+ ≈ 200. For the test DEBORA1 a grid refinement study was performed which showed no change of the results until this value of y+ has decreased to about 70. For still smaller values no convergence could be achieved. This

is a well-known problem of the Kurul and Podowsky (1990, 1991) wall boiling model where all vapour generation occurs in the grid cell adjacent to the wall.

4.2. Calibration of model parameters

For the present case, the experimentally determined profiles of bubble sizes at the end of the heated length are used to estimate suitable parameter values for the detachment bubble size. It turns out that depending on the system pressure different parameter values have to be used in the simulations. The values for the bubble size at detachment in Eq. (2) are estimated from the outermost measurement points of the experimental bubble size profiles. The values used in the present simulations are summarized in Table 3 and compared with the values calibrated to the Bartolomej (1967) tests. Evidently the bubbles are much smaller in the DEBROA tests.

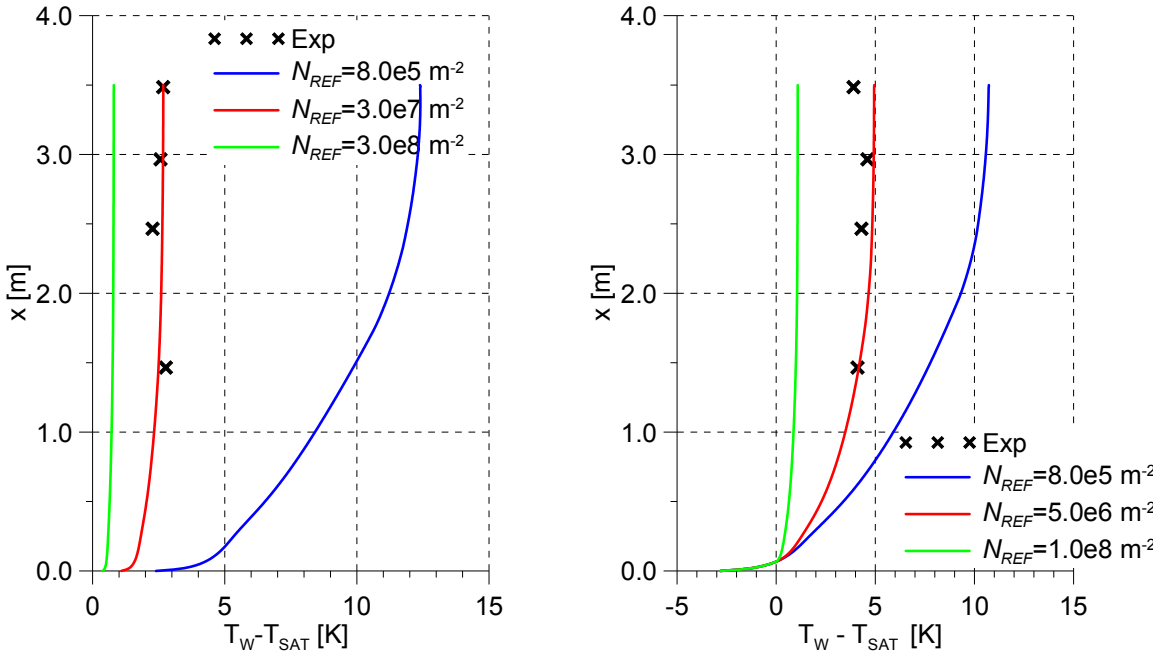

a) P = 2.62 MPa (DEBORA1) b) P = 1.46 MPa (DEBORA4)

Figure 3: Wall superheat depending on the nucleation site density N_{ref}[m^{-2}].

The nucleation site density N has a strong influence on the boiling model results, most notably on the wall superheat T_W -T_{sat}. Unfortunately from the experiments no information about nucleation site density values is available. Therefore, this value is adjusted to obtain agreement with the measured axial profiles of wall superheat. The calculated superheat profiles for several different values of N are compared to the measurements for the tests DEBORA1 and DEBORA4 in Fig. 3a and Fig. 3b, respectively. The value of N_{ref} in Eq. (3) adjusted to the Bartolomej (1967) measurements, $N_{ref} = 0.8\ 10^6$ m^{-2}, yields much too high superheats, but with increasing N_{ref}, the calculated wall superheat decreases. Values of $N_{ref} = 3.0\ 10^7$ m^{-2} for a pressure of 2.62 MPa (DEBORA1) and $N_{ref} = 5.0\ 10^6$ m^{-2} for a pressure of 1.46 MPa (DEBORA4) give good agreement with the respective data (see Fig. 3). These values for N_{ref} yield also for each other tests at the corresponding pressure level good agreement of measured and calculated wall superheating temperature.

As shown in Fig. 2 the lift force changes its sign at a certain bubble size that depends on the system pressure. Values of this critical bubble size are 1.0 mm for 2.62 MPa and 1.5 mm for 1.46 MPa. If bubble sizes larger than the critical value occur it becomes necessary to use an inhomogeneous MUSIG approach with at least two velocity groups in order to correctly capture the effects of the lift force. In cases where the bubble size never exceeds the critical value it is possible to use the simpler and computationally less expensive homogeneous MUSIG approach.

Examination of the measured bubble sizes shows that these are lower than the critical value for the tests DEBORA1 and DEBORA2 with P = 2.62 MPa. Therefore a homogeneous MUSIG approach employing 15 size groups in the range of 0 to 1.5 mm was applied for these tests. For the test DEBORA7, however measured bubble sizes larger than the critical value occur. Therefore for the tests DEBORA3 to DEBORA7, where 1.46 MPa, an inhomogeneous approach with two velocity groups for bubbles smaller respectively larger than 1.5 mm and 15 size groups from 0 to 1.5 mm and 20 size groups from 1.5 to 3.5 mm was applied.

Bubble size profiles for selected values of the calibration parameters F_C and F_B were introduced. The best matching values to the measurements are summarized in Table 3. It is seen that once again a single set of parameter values can be applied for the same pressure level.

Table 3: Adapted parameters related to system pressure

Tests	P	d_{ref}, Eq. (7)	N_{ref}, Eq. (8)	F_B	F_C
Bartolomej	4.7 MPa	0.6 mm	$8.0 \cdot 10^5$ m^{-2}	-	-
DEBORA 1 - 2	2.62 MPa	0.24 mm	$3.0 \cdot 10^7$ m^{-2}	0.0625	0.5
DEBORA 3 - 7	1.46 MPa	0.35 mm	$5.0 \cdot 10^6$ m^{-2}	0.02	0.5

5. RESULTS

5.1. Development of the bubble size in the bulk

Previous models for the bubble size in the bulk used a monodisperse approach with bubble size parametrized by the liquid temperature (Krepper and Rzehak 2011). For this model with the heat source at the wall the liquid temperature and consequently the simulated bubble size decreases with increasing distance from the wall (Fig. 5, blue line). In the measured bubble size profiles in contrast, an increase of the bubble size with increasing distance from the wall can be observed. The population balance approach introduced in the present work is able to describe at least the correct trends (Fig. 5, red line). Bubble size distributions are shown in Fig. 6 for four different points at the end of the heated length. The point P_1 is located close to the pipe wall, P_2 at a wall distance of 0.003 m, P_3 at about half of the pipe radius and P_4 near the pipe centre. At the nearest position close to the wall P_1 a quite narrow bubble size distribution was found since the bubbles are assumed to leave the heated wall with the detachment diameter d_W (see eq. 2). With increased distance from the wall for the points P_2 to P_4 a shift of the maximum bubble size towards larger values can be observed. Obviously the effect of increasing the average bubble size by coalescence exceeds the effect of bubble shrinking due to condensation. At the same time broadens the size distribution with increasing wall distance.

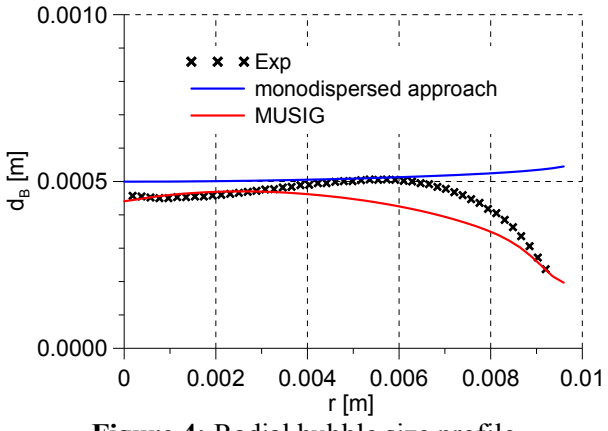

Figure 4: Radial bubble size profile

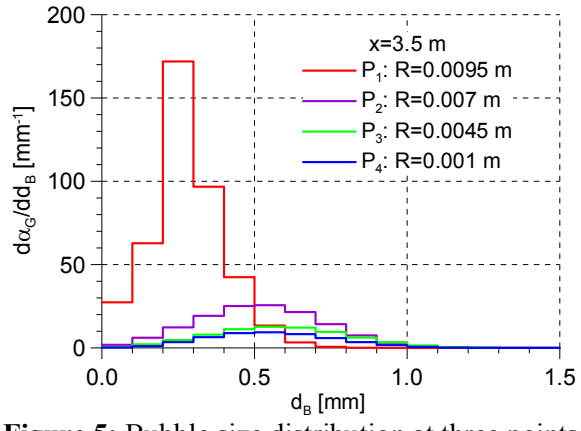

Figure 5: Bubble size distribution at three points

5.2. The gas volume fraction profiles: DEBORA 3 to 7

In the test DEBORA 7 (T_{SUB}=14 K) the measured bubble size (Fig. 6a) almost exceeds the critical value of 1.5 mm, where the lift force changes the sign (see Fig. 2). Therefore for the experimental test series DEBORA3 to DEBORA7 with increasing inlet temperature an inhomogeneous MUSIG approach with two velocity groups was applied. The first velocity group (GAS1) represents 15 equidistant bubble size groups from 0 to 1.5 mm, the second one (GAS2) represents another 20 equidistant bubble size groups from 1.5 to 3.5 mm. Model parameters have been kept at the single values as determined in section 4 for all tests.

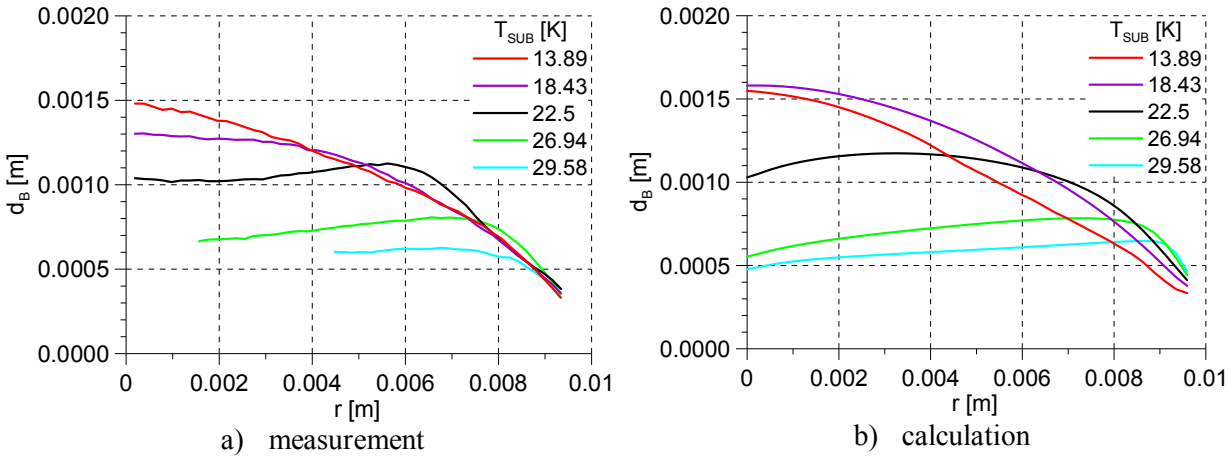

Figure 6: Radial profiles of the bubble size (P=1.46 MPa)

Comparing the measured radial gas volume fraction profiles for the test series DEBORA3 to DEBORA7 with increasing inlet temperature respective decreasing subcooling temperature a shift from wall peak (DEBORA3) to core peak (DEBORA7) can be observed (see Fig. 7a). This phenomenon could not be captured by the monodisperse model approach of Krepper and Rzehak (2011).

As can be seen in Fig. 7b, the models applied here are able to describe the bubble size profiles quite well and at least the tendency of the observed shift of the gas volume fraction maximum is reproduced. It can be seen that as the gas volume fraction peak shifts to the core, the variation of the bubble size across the pipe radius increases so that the radially averaged bubble size that was used in the monodisperse treatment of Krepper and Rzehak (2011) becomes less representative of the true profile.

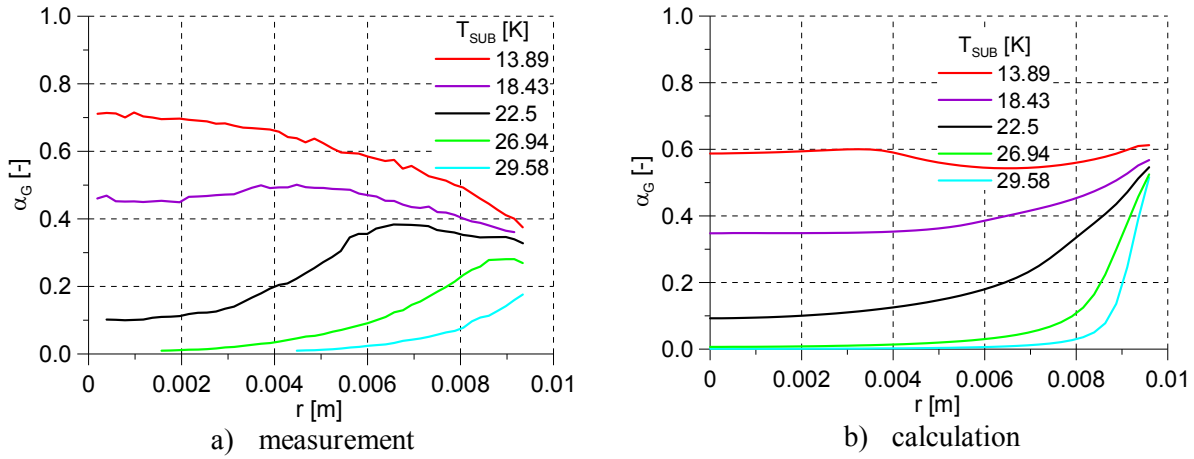

Figure 7: Radial profiles of the gas volume fraction (P=1.46 MPa)

A plausible mechanism transporting the gas towards the pipe center is the lift force which changes its direction for large bubbles. This could explain the transport of larger bubbles into the pipe centre. In the Figs. 8a and 8b the contributions of the individual gas phases representing the different velocity groups are presented. For the group representing the small bubbles (Fig 8a) in all cases a wall peaking profile can be observed due to the lift force pushing these bubbles towards the wall. For the group representing the large bubbles (Fig 8b), because of the opposite direction of the lift force, in all cases a radial gas volume fraction profile showing a core peak is observed. With increasing inlet temperature the share of the gas phase representing large bubbles increases and determines the profile shape of the total gas volume fraction. The mechanism becomes evident also in the two-dimensional gas volume fraction fields shown in Fig. 9. The right panel shows the location of gas contained in bubbles with size d_B < 1.5 mm is mainly near the heated wall. The middle panel gives the corresponding result for bubbles with size d_B > 1.5 mm, which can be found mainly in the core. The total gas volume fraction (left panel) produces a core maximum at the end of the heated length.

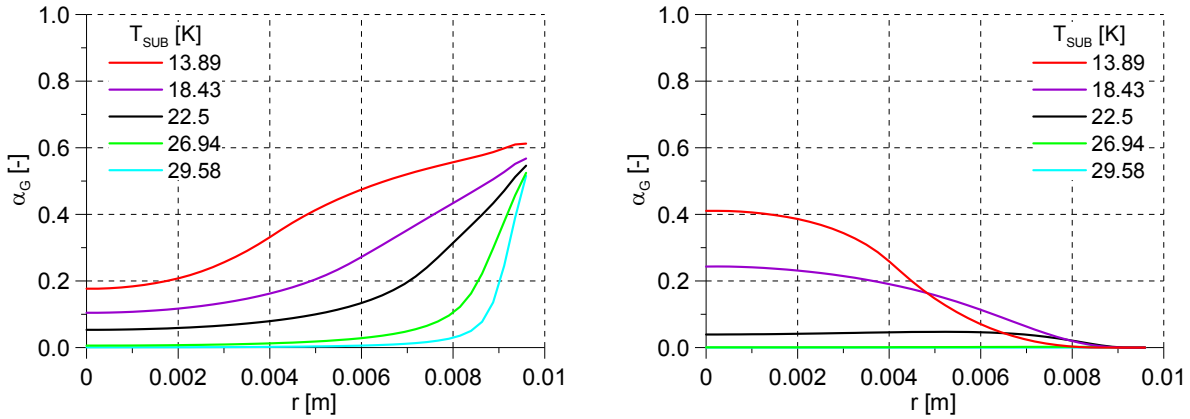

a) Volume fraction GAS1 (d_B<1.5 mm) b) Volume fraction GAS2 (d_B>1.5 mm)

Figure 8: Calculated radial profiles of the gas volume fraction (P=1.46 MPa)

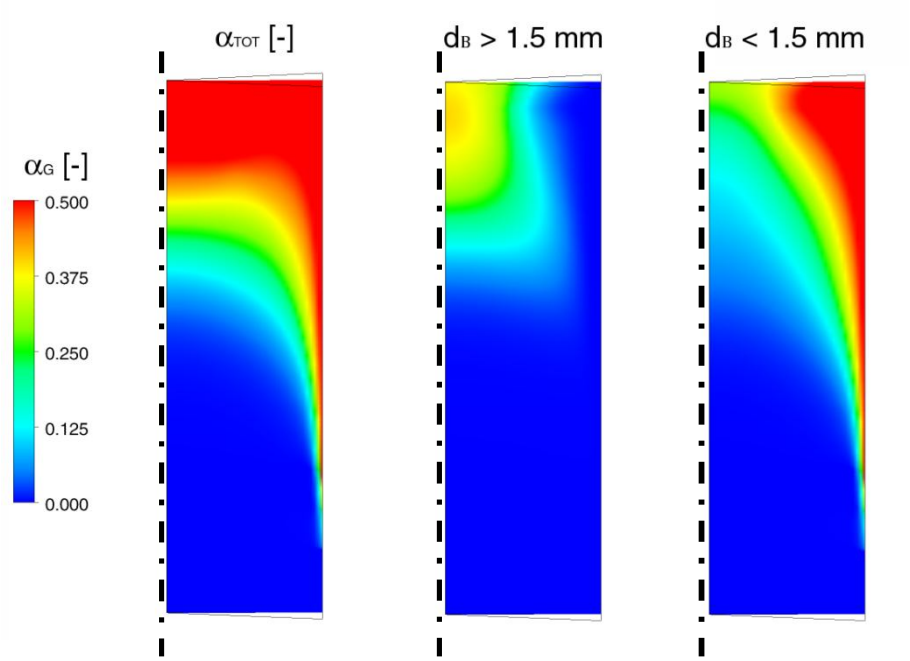

Figure 9: Two-dimensional gas volume fraction fields in the pipe for the test DEBORA7 (pipe length presented shortened)

6. SUMMARY AND CONCLUSIONS

Boiling at a heated wall has been simulated by an Euler / Euler description of two-phase flow combined with a heat flux partitioning model describing the microscopic phenomena at the wall by empirical correlations adapted to experimental data. At the same time the bubble size distribution in the bulk was described by a population balance approach by coupling the wall boiling model with the MUSIG model.

Some of the parameters used in these correlations have to be carefully recalibrated for the present application. The DEBORA tests provide a large body of information that can be used to this end. Quantities with a strong influence on the amount of produced steam are the bubble size at detachment and the nucleation site density. The former can be taken straight forwardly from the measurements. On the latter unfortunately no direct information is available, however, by matching the temperature of the heated wall, this gap can be closed. In both cases the recalibration results in different values for different pressure levels. It was shown, that for the same pressure condition the parameter set adapted to a certain test can be applied to other tests with equally good agreement.

The measured gas bubble size profiles show an increase of the bubble size with increased distance from the heated wall. A monodispersed treatment is not able to capture this phenomenon but including polydispersity by means of a MUSIG approach and suitable models especially for bubble coalescence this phenomenon can be described. Moreover, a shift of the gas volume fraction profile from a wall peak to a core peak has been observed for a test series with increasing inlet temperature. Again this phenomenon could not be captured by a model with a monodisperse bubble size, but can be described using an inhomogeneous MUSIG approach. Here, bubbles of different size are allowed to move with different velocities and in different directions in response to the bubble size dependent lift force.

A complete polydispersed description requires that processes of coalescence / breakup and condensation / evaporation must be modelled explicitly. In the present work the commonly applied models for bubble coalescence according to Prince and Blanch (1990) respective for bubble breakup according to Luo and Svenson (1996) were used as a first step. To reach a fair agreement with the measurements, calibration factors had to be introduced, each valid for a certain pressure level. In this way the suitability of the general model framework could be demonstrated in principle. For a trusted prediction further development of the coalescence and breakup models is necessary.

Bubble coalescence and breakup are heavily influenced by two phase flow turbulence. Unfortunately in the literature only few measurements of turbulent characteristics of two phase flow can be found and even less when boiling occurs. Furthermore, models of bubble-induced turbulence working well for air/water flow may fail for steam/water flow at higher pressure or for refrigerants. In the present work the selection of a specific model for bubble effects on the turbulence is confirmed mainly by plausibility of the final results. Hence, a more systematic investigation of approaches to modelling bubbly turbulence would be desirable.

Finally, looking carefully at the figures showing the gas volume fraction profiles in the near wall region the calculated gas volume fraction is systematically too large. This is particularly evident in the cases with the pressure of 1.46 MPa. Reasons could be a missing force pushing the bubbles away from the wall or the neglect of swarm effects in the models of drag and lift forces even at gas volume fractions around 50%. Furthermore, the application of the simple heat transfer correlation of Ranz and Marshall (1952) might be questionable. In transferring models used successfully for adiabatic air/water flows to the DEBORA tests it should be noted that bubbles are much smaller here which may require changes beyond simple recalibration of parameters.

Overall, our results confirm the great potential of the Euler / Euler two-phase flow and heat flux partitioning models for the simulation of subcooled flow boiling in industrial applications while at the same time highlighting the need for specific model improvements in order to achieve highly accurate quantitative predictions.

7. ACKNOWLEDGEMENT

This work is funded by the Federal Ministry of Education and Research (contract n° 02NUK010A).

8. REFERENCES

Bartolomej, G.G., Chanturiya, V.M., 1967. Experimental study of true void fraction when boiling subcooled water in vertical tubes, *Thermal Engineering* Vol. 14, pp. 123-128, translated from Teploenergetika Vol. 14, 1967, 2, pp. 80-83

Boucker, M., Guelfi, A., Mimouni, S., Péturaud, P., Bestion, D., Hervieu, E., 2006. Towards the prediction of local thermal-hydraulics in real PWR core conditions using NEPTUNE_CFD software, *Workshop on Modeling and Measurements of Two-Phase Flows and Heat Transfer in Nuclear Fuel Assemblies*, KTH, Stockholm, Sweden - 10-11 October 2006

Burns, A.D., Frank, T., Hamill, I., Shi, J.-M., 2004. The favre averaged drag model for turbulence dispersion in Eulerian multi-phase flows, 5th Int. Conf. on Multiphase Flow, ICMF'2004, Yokohama, Japan, 2004.

Cieslinski, J. T.; Polewski, J., Szymczyk, J. A. 2005. Flow Field around Growing and Rising Vapour Bubble by PIV Measurement, *Journal of Visualization*, 8, 209

Frank, T.; Zwart, P.; Krepper, E.; Prasser, H.-M., Lucas, D., 2008. Validation of CFD models for mono- and polydisperse air–water two-phase flows in pipes, *Nuclear Engineering and Design*, 238, 647-659

Garnier, J., Manon, E., Cubizolles, G. 2001. Local measurements on flow boiling of refrigerant 12 in a vertical tube, *Multiphase Science and Technology,* 13, pp. 1-111

Han, C.-Y., Griffith, P., 1965. The Mechanism of Heat Transfer in Nucleate Pool Boiling*, Int. J. Heat Mass Transfer*, 8, 887

Ishii, M., Zuber, N., 1979. Drag coefficient and relative velocity in bubbly, droplet or particulate flows, AIChE J. 25, 843-855

Kader, B.A. 1981. Temperature and concentration profiles in fully turbulent boundary layers, *Int. J. Heat Mass Transfer* 24, pp. 1541-1544.

Krepper, E., Rzehak, R., 2011. CFD for subcooled flow boiling: Simulation of DEBORA experiments, *Nuclear Engineering and Design*, 241, 3851– 3866

Krepper, E.; Beyer, M.; Lucas, D. & Schmidtke, M. 2011a. A population balance approach considering heat and mass transfer - Experiments and CFD simulations, *Nuclear Engineering and Design* 241, 2889-2897

Krepper, E., Lucas, D., Frank, T., Prasser, H.-M., Zwart, P. 2008. The inhomogeneous MUSIG model for the simulation of polydispersed flows, *Nuclear Engineering and Design*, 238, 1690–1702

Kurul, N., Podowski, M.Z., 1990. Multidimensional effects in forced convection subcooled boiling, Proc. 9th Int. Heat Transfer Conf., Jerusalem, Israel

Kurul, N., Podowski, M., 1991. On the modeling of multidimensional effects in boiling channels ANS Proceedings of 27th National Heat Transfer Conference, Minneapolis, MN

Lifante, C., F. Reiterer, Th. Frank, A. Burns (2011) Coupling of wall boiling with discrete population balance model, *The 14th International Topical Meeting on Nuclear Reactor Thermalhydraulics*, NURETH-14, Toronto, Ontario, Canada, September 25-30, 2011, NURETH14-087

Lucas, D., M., Frank, T., Lifante, C, Zwart, P., Burns, A., 2011. Extension of the inhomogeneous MUSIG model for bubble condensation. *Nuclear Engineering and Design* 241, 4359–4367

Lucas, D., Prasser, H.-M. 2007a. Steam bubble condensation in sub-cooled water in case of co-current vertical pipe flow, Nuclear Engineering and Design, 237, 497-508

Lucas, D., Krepper, E., Prasser, H.-M., 2007b. Use of models for lift, wall and turbulent dispersion forces acting on bubbles for poly-disperse flows. Chem. Eng. Science 62, 4146-4157.

Lucas, D. & Krepper, E., 2007c. CFD models for polydispersed bubbly flows, Forschungszentrum Dresden, FZD-486

Luo, H., Svendsen, H.F., 1996. Theoretical model for drop and bubble break-up in turbulent flows, AIChEJ, 42, 5, pp. 1225-1233

Manon, E. 2000. Contribution à l'analyse et à la modélisation locale des écoulements boillants sous-saturés dans les conditions des Réacteurs à Eau sous Pression, PhD thesis, Ecole Centrale Paris, Nov. 2000

Menter F., 1994. Two-equation eddy-viscosity turbulence models for engineering applications, AIAA-Journal, Vol. 32, No. 8.

Politano, M., Carrica, P., Converti, J., 2003. A model for turbulent polydisperse two-phase flow in vertical channels, *International Journal of Multiphase Flow*, 29, 1153

Prince, M.J., Blanch, H.W., 1990. Bubble coalescence and break-up in air-sparged bubble columns, AIChEJ, 36, No 10, pp. 1485-1499

Sato, Y., Sadatomi, M., Sekoguchi, K., 1981. Momentum and heat transfer in two-phase bubble flow-I, *Int. J. of Multiphase Flow*, vol. 7, pp. 167-177, 1981.

Schmidtke, M., 2008. Investigation of the dynamics of fluid particles using the Volume of Fluid Method, PhD-Thesis University Paderborn, (in German)

Tolubinsky, V.I., Kostanchuk, D.M., 1970. Vapour bubbles growth rate and heat transfer intensity at subcooled water boiling; Heat Transfer 1970, Preprints of papers presented at the 4^{th} *International Heat Transfer Conference*, Paris, Vol. 5, Paper No. B-2.8

Tomiyama, A., Tamai, H., Zun, I., Hosokawa, S., 2002. Transverse migration of single bubbles in simple shear flows, *Chemical Engineering Science*, 2002, 57, 1849-1858

Wellek, R.M., Agrawal, A.K., Skelland, A.H.P., 1966. Shapes of liquid drops moving in liquid media, AIChE Journal, vol. 12, pp. 854-860

Yao, W., Morel, C., 2002. Prediction of parameters distribution of upward boiling two-phase flow with two-fluid models, 10th International Conference on Nuclear Engineering ICONE-10-22463, Arlington, April 14-18